RESEARCH PAPER

CrossMark

An inconvenient truth about xylem resistance to embolism in the model species for refilling *Laurus nobilis* L.

Laurent J. Lamarque[1,2] · Déborah Corso[2] · José M. Torres-Ruiz[2] · Eric Badel[3] · Timothy J. Brodribb[4] · Régis Burlett[2] ·
Guillaume Charrier[2,5] · Brendan Choat[6] · Hervé Cochard[3] · Gregory A. Gambetta[5] · Steven Jansen[7] · Andrew King[8] ·
Nicolas Lenoir[9] · Nicolas Martin-StPaul[10] · Kathy Steppe[11] · Jan Van den Bulcke[12] · Ya Zhang[7] · Sylvain Delzon[2]

Abstract

• *Key message* Direct, non-invasive X-ray microtomography and optical technique observations applied in stems and leaves of intact seedlings revealed that laurel is highly resistant to drought-induced xylem embolism. Contrary to what has been brought forward, daily cycles of embolism formation and refilling are unlikely to occur in this species and to explain how it copes with drought.

• *Context* There has been considerable controversy regarding xylem embolism resistance for long-vesselled angiosperm species and particularly for the model species for refilling (*Laurus nobilis* L.).

• *Aims* The purpose of this study was to resolve the hydraulic properties of this species by documenting vulnerability curves of different organs in intact plants.

• *Methods* Here, we applied a direct, non-invasive method to visualize xylem embolism in stems and leaves of intact laurel seedlings up to 2-m tall using X-ray microtomography (microCT) observations and the optical vulnerability technique. These approaches were coupled with complementary centrifugation measurements performed on 1-m long branches sampled from adult trees and compared with additional microCT analyses carried out on 80-cm cut branches.

• *Results* Direct observations of embolism spread during desiccation of intact laurels revealed that 50% loss of xylem conductivity (Ψ_{50}) was reached at -7.9 ± 0.5 and -8.4 ± 0.3 MPa in stems and leaves, respectively, while the minimum xylem water potentials measured in the field were -4.2 MPa during a moderate drought season. Those findings reveal that embolism formation is not routine in *Laurus nobilis* contrary to what has been previously reported. These Ψ_{50} values were close to those based on the flow-centrifuge technique (-9.2 ± 0.2 MPa), but at odds with microCT observations of cut branches (-4.0 ± 0.5 MPa).

Laurent J. Lamarque and Déborah Corso contributed equally to this work.

Handling editor: Erwin Dreyer

Electronic supplementary material The online version of this article (https://doi.org/10.1007/s13595-018-0768-9) contains supplementary material, which is available to authorized users.

✉ Sylvain Delzon
sylvain.delzon@u-bordeaux.fr

Extended author information available on the last page of the article

INRA
SCIENCE & IMPACT

Springer

• **_Conclusion_** In summary, independent methods converge toward the same conclusion that laurel is highly resistant to xylem embolism regardless its development stage. Under typical growth conditions without extreme drought events, this species maintains positive hydraulic safety margin, while daily cycles of embolism formation and refilling are unlikely to occur in this species.

1 Introduction

Increases in temperature and shifts in rainfall are expected to change the severity and frequency of drought events worldwide (Dai 2013; Fields et al. 2012). Forests are highly vulnerable to such changes in climate as drought decreases both plant growth and survival (Barigah et al. 2013; Cailleret et al. 2017; Hogg et al. 2008; Michaelian et al. 2011; Sanchez-Salguero et al. 2012). Global observations of increasing drought-induced forest damage have already been reported (Allen et al. 2010, 2015), while extreme climatic events are projected to be more frequent in the next decades (Diffenbaugh et al. 2015; Jentsch et al. 2007; Meehl and Tebaldi 2004). Global forest diebacks pose a serious threat to biodiversity and ecosystem services (Anderegg et al. 2016), and improving their forecasting via a better representation of plant drought resistance in dynamic vegetation models is critical (Anderegg et al. 2015; Lindenmayer et al. 2012). However, this is only possible through a proper understanding of the mechanisms underlying plant resistance to water stress.

Recent advances in plant hydraulics have highlighted the close link between drought-induced mortality and resistance to xylem embolism (Brodribb and Cochard 2009; Brodribb et al. 2010; Choat et al. 2012; Urli et al. 2013; Urli et al. 2014). As the portion of embolized conduits increases, xylem hydraulic conductivity decreases until water flow stops, inducing plant tissue desiccation (Sperry and Pockman 1993) and ultimately death (Barigah et al. 2013). Global surveys of plant vulnerability to drought have shown that plants from xeric environments are, on average, more resistant to xylem embolism than species from wetter climates (Choat et al. 2012; Cochard et al. 2008; Maherali et al. 2004). However, debate has arisen regarding the ability of some techniques to accurately evaluate resistance to xylem embolism, with studies arguing for their soundness (Hacke et al. 2015; Sperry et al. 2012; Tobin et al. 2013), while others have indicated the existence of artifacts (Choat et al. 2010; Cochard et al. 2010; Torres-Ruiz et al. 2014; Wheeler et al. 2013). This has led to major discrepancies in the interpretation of results (Cochard and Delzon 2013; Jansen et al. 2015; Rockwell et al. 2014), especially as uncertainties remain regarding the water potential of xylem tissues where refilling has been observed (Brodersen et al. 2010; Charrier et al. 2016; Clearwater and

Goldstein 2005). Plants can be considered highly resistant to hydraulic failure, which likely occurs only under severe water stress (Brodribb et al. 2010; Choat et al. 2016; Delzon and Cochard 2014). An alternative hypothesis is that plants show a low-embolism resistance and high repair capacity, suggesting the refilling of conduits without the prerequisite of root/stem pressure (Knipfer et al. 2016; Nardini et al. 2008; Trifilò et al. 2014a).

In this context, there is an urgent need to accurately evaluate drought-induced xylem embolism formation and repair by real-time, non-invasive methods, avoiding possible artifacts during measurements. Two state-of-the-art methods offer such an opportunity: (i) X-ray microtomography (microCT), which has been proven to be a sound method to directly visualize, at high resolution, the amount of embolized vessels (Brodersen et al. 2010; Choat et al. 2016; Cochard et al. 2015; McElrone et al. 2013; Nolf et al. 2017) and the pattern of embolism spread in intact plants (Torres-Ruiz et al. 2016) and (ii) the optical vulnerability technique (Brodribb et al. 2016a, b), which allows real-time visualization of leaf embolism in situ.

The controversies surrounding hydraulic measurements and their interpretation are best exemplified by the case of laurel (_Laurus nobilis_ L.), a long-vesseled Mediterranean species. Two decades of experiments have not produced a consensus regarding the resistance of this species to drought-induced xylem embolism or its ability to refill embolized conduits. Based on techniques, such as bench dehydration (Hacke and Sperry 2003; Salleo and Lo Gullo 1993; Salleo et al. 2000; Trifilò et al. 2014a), air injection (Salleo et al. 1996, 2004; Tyree et al. 1999), and centrifugation (Cochard 2002), laurel undergoes 50% loss of hydraulic conductivity (Ψ_{50}) at xylem pressures ranging from − 1.5 (Salleo et al. 2009) to − 2.4 MPa (Cochard 2002; Salleo and Lo Gullo 1993). As a result, laurel has been thought to be highly vulnerable to embolism. Indeed, this has been supported by the fact that additional experiments reported the presence of embolism repair mechanisms, such as daily vessel refilling, which would allow the species to endure the regular water stress periods that characterize Mediterranean plants (Salleo et al. 1996; Trifilò et al. 2014a, b; Tyree et al. 1999). However, there is no direct, visual evidence for embolism repair in intact laurel plants (Knipfer et al. 2017), while many measurements on _L. nobilis_ may suffer from

artifacts associated with cutting stems prior to measurement (Torres-Ruiz et al. 2015; Wheeler et al. 2013). Both the "open-vessel" and "cutting" artifacts may lead to an overestimation of embolism when using standard hydraulic methods to determine vulnerability of long-vesseled species (Choat et al. 2010; Cochard et al. 2010; Torres-Ruiz et al. 2017; Wheeler et al. 2013). Direct microCT observations also showed that the pressures inducing embolism in xylem vessels of excised laurel shoots were below − 3 MPa, with only 30% loss of hydraulic conductivity reached at − 6 MPa (Cochard et al. 2015). This view was questioned by Nardini et al. (2017), whose microCT based vulnerability curve for cut laurel segments was similar to those previously determined with classical hydraulic measurements, showing 50% loss of hydraulic conductance at a xylem pressure of − 3.5 MPa.

The lack of consensus regarding vulnerability to embolism in long-vesseled species, such as laurel, may result from the fact that until now both hydraulic techniques and direct visualization have mainly been conducted on cut branches. The purpose of this study was to resolve the hydraulic properties of this species by documenting vulnerability curves of different organs in intact plants. Our approach was twofold: (i) determining stem vulnerability to embolism by scanning intact laurel seedlings at microCT facilities and (ii) quantifying leaf vulnerability to embolism of intact plants using the optical vulnerability technique (Brodribb et al. 2016a, b). Those non-invasive and real time assessments of drought-induced embolism were finally coupled with flow-centrifuge measurements conducted on 1-m long branches and supposed to overcome the open-vessel artifact. The results provide novel information about the resistance to embolism for this species and indirectly evaluate whether embolism formation and repair occur routinely, i.e., at low xylem tensions.

2 Material and methods

2.1 Stem vulnerability to embolism

2.1.1 X-ray microtomography

Direct visualizations of embolized xylem vessels in the main stems of intact laurel plants were carried out during two tomography campaigns. The first was conducted in August 2015 at the Centre for X-ray Tomography of Ghent University (UGCT; Belgium), while the second was undertaken in May 2016 at the SOLEIL Synchrotron (France).

For the first campaign, 20 1-year-old seedlings from PlanFor nursery (Uchacq-et-Parentis, France) were reported in May 2015 into 1-L pots and grown for 2 months under well-watered conditions at the facilities of Ghent University. During the experiment, eight seedlings were uprooted with bagged roots and leaves to avoid water losses by transpiration. At the time of scanning, laurel individuals were 0.3-m tall and 3- to 5-mm wide at the stem base. Tomographic observations were conducted using the High-Energy CT system Optimized for Research (HECTOR scanner), which was equipped with a 240-kV X-ray tube (X-ray WorX, Garbsen, Germany) and a 1620 flat-panel detector (PerkinElmer, Waltham, MA, USA) (Masschaele et al. 2013). Plants were installed on a stage immobilizing the stems and scanned just above soil surface at 90 kV. Each scan took ca. 25 min for each sample and yielded a stack of 2000 TIFF image slices. On average, each stem section was scanned three times at different levels of dehydration as repeated scans at the same scan point have been shown to not cause cavitation in dehydrating samples (Choat et al. 2016). The scans were reconstructed with the Octopus Reconstruction software package (Dierick et al. 2004; Vlassenbroeck et al. 2007; licensed by InsideMatters: www.insidematters.eu), providing images with a 5.12-μm^3 voxel resolution.

The second set of tomographic observations was conducted at the SOLEIL microCT PSICHÉ beamline (King et al. 2016). The main stem of six 3-year-old and 2-m tall intact laurels from Le Lann nursery (Gradignan, France) was scanned using a high flux (3.10^{11} photons mm^{-1}) 25-keV monochromatic X-ray beam, while being rotated from 0° to 180° using a continuous rotation mode. Thanks to the high load capacity and free central aperture of the rotation stage, imaging cross sections were also selected near the middle of the main stems, i.e., at 1 m above the stem base. Dehydration was progressively induced in the six plants by stopping irrigation and exposing them to a fan to accelerate the process. X-ray projections were collected with a 50-ms exposure time during rotation and recorded with an Orca-flash sCMOS camera (Hamamatsu Photonics K.K., Naka-ku, Japan) equipped with a 250-μm thick LuAG scintillator. The scan time was 75 s for each sample and yielded a stack of 1500 TIFF image slices. Each stem section was scanned at the same location two to three times throughout dehydration of the laurel individuals. Tomographic reconstructions were conducted using the Paganin method (Paganin et al. 2002) in PyHST2 software (Mirone et al. 2014) and resulted in 2-bit volumic images with a 3.02-μm^3 voxel resolution. Finally, tomography observations at the SOLEIL facility were also conducted on five 80-cm long branches, cut in air from the same set of well hydrated 3-year-old seedlings and left on the laboratory bench to dehydrate. One cross-section was randomly selected at an internode located near the middle of each segment, i.e., ca. 40-cm away from the cut end, and all leaves situated both below and above this internode were preserved.

Stem water potential (Ψ_{stem}) was measured the same way in both campaigns and for both intact plants and cut branches. Specifically, Ψ_{stem} was monitored before each scan ($n = 31$ and

32 for a total of 14 intact plants and five cut branches, respectively) with a Scholander pressure bomb (Model 1000, PMS Instrument, Albany, OR, and SAM Precis, Gradignan, France) using a leaf located below the scanned area and that had been covered for at least 2 h with aluminum foil and wrapped in a plastic bag. We intentionally limited our water potential measurements to measurements on a single leaf located below the scanned area to avoid (i) potential air-entry via cut petioles, which was shown to be an artifact for *Quercus robur* (Choat et al. 2016) and (ii) an underestimation of the water potential at the scan location, since there can be a strong hydraulic disconnection between the base of the stem and the top leaves after a certain amount of xylem embolism (Charrier et al. 2016).

Measurements were conducted for each scan from a transverse cross section taken from the center of the scan volume. The theoretical hydraulic conductivity of a whole cross section (k_h) was determined by calculating the individual area and diameter of both air- and water-filled vessels. Vessel visualization, i.e., the distinction between functional vessels from non-functional xylem conduits and fibers, and vessel diameter calculation were facilitated by using a final scan ("final cut") that was generated for each stem section (Fig. S1). Final cuts represented scans performed after samples were cut in air ca. 2 mm above the corresponding scanned stem volume and where functional vessels with sap under tension immediately filled with air. Measurements were conducted manually with ImageJ software (National Institute of Health, New York, NY, USA), focusing only on secondary xylem given that primary xylem had previously become embolized in most cases (Choat et al. 2016). The theoretical hydraulic conductivity (k_h, $m^2\ MPa^{-1}\ s^{-1}$) of air-filled vessels of each cross section was calculated as:

$$k_h = \Sigma \pi D^4 / 128\eta \tag{1}$$

where D is the diameter of vessels (m) and η is the water viscosity (1.002 $mPa\ s^{-1}$ at 20 °C).

The theoretical loss of hydraulic conductivity (PLC, %) was then determined as:

$$PLC = 100 \cdot (k_h / k_{max}) \tag{2}$$

where k_{max} represents the theoretical hydraulic conductivity of all functional vessels as based on a cross section after the final cut.

2.1.2 In situ flow-centrifuge technique (Cavitron)

Stem vulnerability to embolism was also measured using the Cavitron technique (Cochard 2002; Cochard et al. 2005). Measurements were conducted between March and May 2016 at the high-throughput phenotyping platform for hydraulic traits (Caviplace, University of Bordeaux, Talence, France) on seven branches collected from mature laurel individuals (one branch sampled per individual) growing at the Domaine du Haut-Carré woodland in the University of Bordeaux campus (lat: 44.8089479, lon: − 0.5955238). Prior to the main experiment, we had sampled seven additional branches to assess whether we were able to construct vulnerability curves using either the standard (27-cm large rotor) or the medium (42-cm large rotor) Cavitron. In both cases, the VCs obtained did not present stable values of stem hydraulic conductivity (k_s, $m^2\ MPa^{-1}\ s^{-1}$) at high xylem pressure due to the open-vessel artifact (e.g., length of 20% of vessels exceeded the rotor diameter as described in section 3), and we therefore could not use these curves to estimate the maximum k_s and thus the PLCs (Fig. 1) (Torres-Ruiz et al. 2014, 2017). To overcome this issue, we consequently used a Cavitron which is equipped with a 100-cm diameter rotor

Fig. 1 Vulnerability curves obtained with the standard (27-cm rotor) and medium (42-cm rotor) Cavitrons
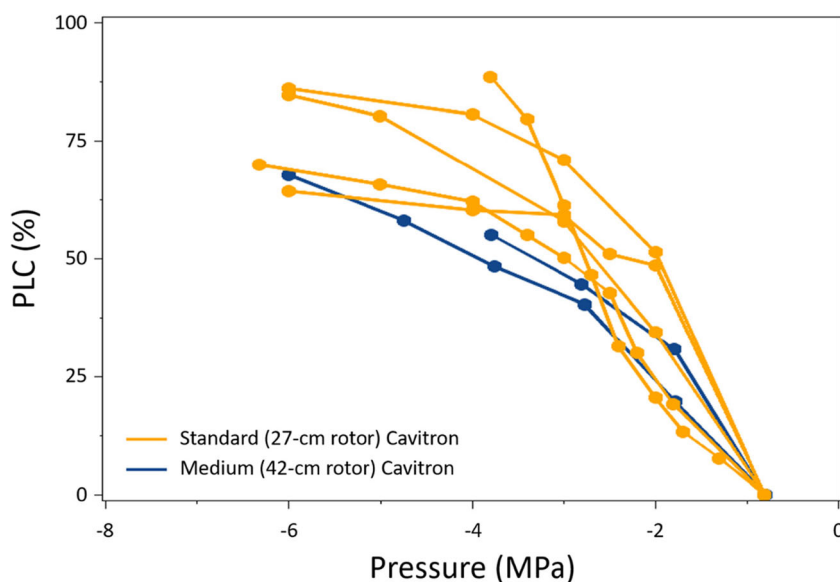
(DG-MECA, Gradignan, France) driven by an electronically controlled motor and which proved successful when testing embolism vulnerability in long-vesseled species, such as grapevine (Charrier et al. 2018). Sampling of 2.5-m long branches was carried out at early morning before transpiration resumes in order to avoid high xylem tensions and to minimize the induction of artifactual xylem embolism (Torres-Ruiz et al. 2015; Wheeler et al. 2013). Stems were wrapped with moist paper and conditioned with plastic bags to avoid any water loss by transpiration. They were immediately brought back to the laboratory where they were kept in water for stem relaxation during ca. 1 h. At the time of measurements, branches were cut under water to a standard length of 1 m, with both ends trimmed with a razor blade and debarked over 15 cm. Samples were not flushed with water in order to avoid possible effects of air-seeding fatigue due to a stretching or degradation of the pit membranes during previous embolism events (Li et al. 2016; Zhang et al. 2017). A solution of ultrapure and deionized water containing 10-mM KCl and 1-mM $CaCl_2$ was used as reference ionic solution. Preliminary tests indicated that no change in k_s was observed between 0 and -2 MPa. Therefore, the centrifuge rotation speed was initially set to induce a xylem pressure of -0.8 MPa before being gradually increased to lower xylem pressures by -0.5 MPa. Hydraulic conductivities at every rotation speed (k_i, $m^2\ MPa^{-1}\ s^{-1}$) were measured using the Cavisoft software (v. 5.2, University of Bordeaux). The percentage loss of hydraulic conductivity (PLC) was determined at each pressure as follows:

$$PLC = 100 \cdot (1 - k_i/k_{max}) \qquad (3)$$

where k_{max} represents the maximum hydraulic conductivity measured at the first induced xylem pressure.

2.2 Leaf vulnerability to embolism

The accumulation and spread of embolism in leaves throughout dehydration were monitored between February and April 2016 on four 3-year-old and 2-m tall potted laurels that came from the same set of plants used at the SOLEIL Synchrotron. Seedlings were kept well-hydrated prior to measurements. During the experiment, the intact laurel seedlings were uprooted with bagged roots and leaves to avoid water loss by transpiration. Bags were removed once the scanned leaf and the psychrometers (see below) were installed. Embolism formation was recorded in dehydrating leaves using the optical method (see www.opensourceov.org for details and overview). For each individual, a mature leaf attached to the parent plant was placed on a scanner (Perfection V800 Photo, EPSON, Suwa, Japan) and fixed with a transparent glass and adhesive tape to avoid as much leaf shrinkage as possible during plant desiccation. Scan magnification was set with

the Epson scanner software to give sufficient resolution of both midrib and at least eight major (second order) veins. The following settings were selected: film (with film area guide) as document type, color positive film as document source, 8-bit grayscale as image type, and a 2400-dpi resolution. Brightness and contrasts as well as leaf scanned area were adjusted to optimize visualization of embolism events and provide images not exceeding 9 Mb each. Each leaf was automatically scanned every 3 min using a computer automation software (AutoIt 3) until mesophyll cells were observed to turn from green to brown indicating cell death. Intact laurels were considered dead after 4 to 11 days of desiccation in a room heated at 26 °C when we observed permanent and pronounced leaf damage, which occurred at $\Psi_{leaf} < -9$ MPa. At the end of optical measurements, the stacks of captured images comprised 1915 to 5509 scans.

Stem and leaf water potential were continuously monitored throughout plant dehydration using psychrometers (ICT International, Armidale, NSW, Australia), which were respectively installed on the main seedling stem (Ψ_{stem}) and on a leaf (Ψ_{leaf}) adjacent to the scanned one. Ψ_{stem} and Ψ_{leaf} were automatically recorded every 30 min. The accuracy of psychrometer readings was also cross-validated four to six times a day by Ψ_{leaf} measurements on adjacent leaves that had been covered for at least 2 h with aluminum foil and wrapped in a plastic bag using a Scholander pressure bomb (SAM Precis, Gradignan, France).

Stacks of images were analyzed using ImageJ software. The "StackReg" function was first used to align the scan sequence, i.e., to reduce leaf movements which occurred during desiccation. The image subtraction method was then applied to reveal changes in light transmission between successive images, which corresponded to embolism in xylem conduits of leaf veins. A new stack of images was created, from which three "Regions Of Interest" were drawn, corresponding to the different vein orders studied, namely midrib, major (second) and minor (third and lower order) veins. After smoothing all images, the "Analyze Particles" function was used to measure the area of embolized pixels in each image for each vein order. To do so, a threshold of embolized pixels was set, above which pixel numbers and areas were counted for each image. This function also allowed the removal of noise related to leaf mesophyll cell death. All embolized pixels were finally summed for each vein order to determine the spread of embolism over time and represent the maximum percentage of embolized pixels at a given scan time. An optical vulnerability curve was also determined by representing embolism spread as a function of Ψ_{leaf} (see following section).

2.3 Vulnerability curve fitting

Vulnerability curves, corresponding to percentage loss of hydraulic conductivity (for microCT and centrifugation

techniques) or percentage embolized pixels (for the optical vulnerability technique) as a function of stem water potential, were fitted using the NLIN procedure in SAS 9.4 (SAS, Cary, NC, USA) based on the following equation (Pammenter and Van der Willigen 1998):

$$PLC = 100/(1 + \exp(S/25 \cdot (\Psi - \Psi_{50}))) \qquad (4)$$

where Ψ_{50} (MPa) is the xylem pressure inducing 50% loss of hydraulic conductivity and S (% MPa^{-1}) is the slope of the vulnerability curve at the inflection point. The xylem pressures inducing 12% (Ψ_{12}) and 88% (Ψ_{88}) loss of hydraulic conductivity were calculated as follows: $\Psi_{12} = 50 / S + \Psi_{50}$ and $\Psi_{88} = -50 / S + \Psi_{50}$. One vulnerability curve was obtained per individual for each method (i.e., the Pammenter model was fitted on each vulnerability curve in order to get a Ψ_{50} and slope value per individual and subsequently an average value per method), with the exception of the microCT observations on intact laurels for which the curve was generated directly from all the single scans.

2.4 Maximum and mean vessel length

Vessel length was determined for five fresh laurel branches that were similar to those used for the in situ flow-centrifuge measurements mentioned below, using the "air injection" method with slight modification from (Wang et al. 2014). Briefly, compressed air was delivered from an air compressor (Nuair, Saint-Quentin-Fallavier, France) to the basal end of branches (130–250-cm long and 15–20 mm in basal diameter). The incoming air flow (Q, L min^{-1}) from the compressor was measured with an in-line, low pressure drop flow-meter (El-flow select F110, Bronkhorst, The Netherland). The air pressure, set at 1.80 bars (e.g., 15 times below the air-seeding threshold (Jansen et al. 2009), was monitored as the sample distal end was cut to consistent lengths using an analog manometer connected just before the sample basal end. This process took less than 10 min per branch, thus avoiding pit membrane dehydration with shrinkage and artificially enlarged pores as possible consequences. Computation of mean vessel lengths was performed from the air flow and sample lengths according to (Cohen et al. 2003).

2.5 Minimum midday water potential (Ψ)

We monitored minimum midday water potentials (Ψ) throughout the summer 2017 on a total of 12 mature laurel individuals growing at the Domaine du Haut-Carré woodland of the University of Bordeaux, including the seven individuals that were sampled for the in situ flow-centrifuge measurements. Ψ measurements were conducted between 12:45 and 13:15 pm on a weekly basis. One leaf located in the tree crown was sampled per individual and immediately placed in a plastic

bag where air was kept saturated to prevent transpiration. Measurements were carried out in the laboratory 10 to 20 min after leaf sampling using a Scholander pressure bomb (SAM Precis, Gradignan, France).

2.6 Statistical analyses

Difference in Ψ_{50}, Ψ_{12}, Ψ_{88}, and S values estimated from the three methods were tested with a one-way analysis of variance and Bonferroni pairwise post hoc tests using the ANOVA procedure in SAS (version 9.4, SAS Institute, Cary, NC, USA).

3 Results

3.1 Maximum and mean vessel length

Vessel length measurements based on the air injection method revealed that the longest vessels for the five sampled branches were 104 ± 7-cm long, with a mean vessel length of 32 ± 3 cm. These results shed light on our inability to properly estimate PLCs using standard (27-cm rotor) or medium (42-cm rotor) Cavitrons as reported in Fig. 1.

3.2 Stem vulnerability to embolism

MicroCT observations on intact laurel plants revealed a low level of "native" embolism (~ 2–13%) down to -6 MPa (Fig. 2; see Fig. S2 for raw images). At more negative Ψ_{stem}, the amount of embolized vessels substantially increased leading to 50% embolism at around -8 MPa (Table 1, Figs. 3 and S3a). There was no difference in the level of embolism between 1- and 3-year-old laurel seedlings from the two experiments (Figs. 2 and S3a). In contrast, microCT observations on cut branches showed (i) up to 50% native embolism at 80 cm above the cut and (ii) that the number of air-filled vessels increased at a much higher water potential, with 20–25% embolism observed at ca. -3 MPa and 80 to 90% around -6 MPa ($F = 10.95$, $P = 0.0297$; Table 1, Figs. 3 and S3b).

Vulnerability curves generated with the in situ flow-centrifuge showed moderate variability among individual trees, with Ψ_{50} ranging from -8.3 to -9.7 MPa (Fig. S4). The sigmoidal shape of the vulnerability curve obtained with the centrifugation technique closely matched that obtained with X-ray microCT ($F = 3.61$, $P = 0.1063$; Table 1, Fig. 3).

3.3 Leaf vulnerability to embolism

None or few embolism events were detected at the beginning of plant dehydration (i.e., at high water potentials; e.g., down to -3 MPa). The spread of embolism was temporally
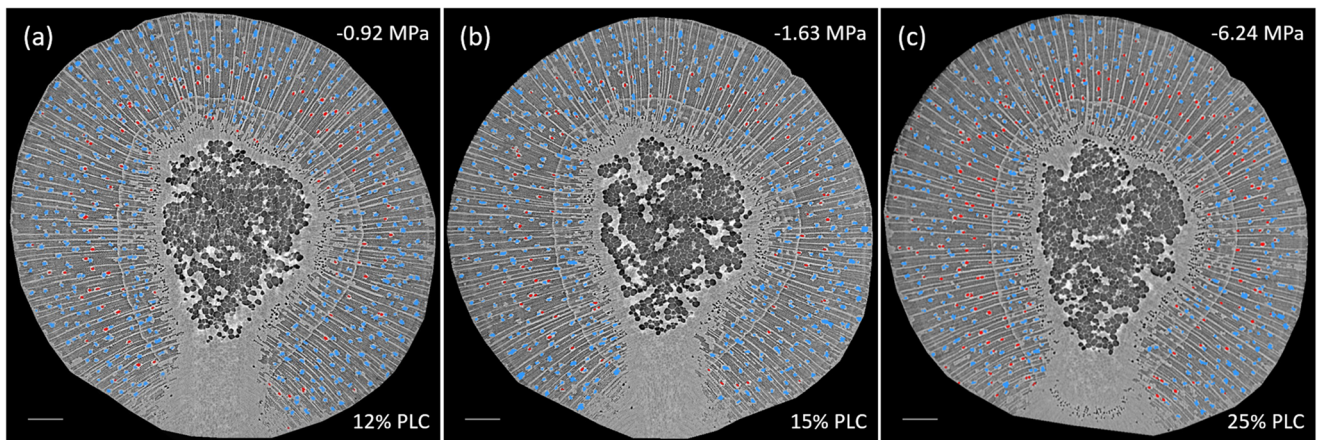
Fig. 2 Visualization by X-ray microtomography (microCT) of xylem embolism in the main stem of a 3-year-old and 2-m tall intact *Laurus nobilis* seedling during dehydration. Images **a**, **b**, and **c** show rates of embolism of 12, 15, and 25% at -0.92, -1.63, and -6.24 MPa, respectively, in transverse stem slices. Embolized vessels were colored in red while water-filled vessels appear in blue. Scale bar = 500 μm. The primary and juvenile xylem near the stem pith was ignored in our analyses. See Fig. S1 for the corresponding final scan and Fig. S2 for corresponding raw images (i.e., without vessels colored)

heterogeneous across laurel individuals: the onset of embolism was recorded 4 to 140 h after uprooting the seedlings (Fig. S5a), while the time needed to produce 12% of embolism (Ψ_{12}) ranged between 53 and 166 h. Despite the large temporal variation in embolism formation between individuals, this variation disappeared when cumulative embolism curves were expressed in terms of water potential (Fig. S5b). While water potential decreased during desiccation, the amount of embolism continuously increased (Fig. S6). The spread of cumulative embolisms followed a sigmoidal function for all individuals when plotted against leaf water potential (Fig. 3). While Ψ_{12} was reached at Ψ_{leaf} ranging from -4.5 to -8.04 MPa, the final embolism events were recorded at Ψ_{leaf} between -8 to -10 MPa (Fig. 4). On average, the vast majority of embolism formation in leaves occurred over a narrow range of Ψ_{leaf}. Overall, water potentials required to induce 50% of the total amount of embolism in leaves of intact laurels were significantly similar to the Ψ_{50} values obtained for the main stems of intact individuals based on microCT ($F = 3.61$, $P = 0.1063$; Table 1; Fig. 3). Embolism was clearly visible in midrib, major, and minor veins, and these all showed similar vulnerability to embolism ($F = 0.08$, $P = 0.9216$; Fig. 5) and experienced multiple embolism events (Fig. 4, as shown by the accumulation of different colors).

3.4 Minimum midday water potential (Ψ)

The 12 mature laurel trees monitored experienced on average minimum midday Ψ values close to -3 MPa during the entire summer of 2017, with some individuals showing Ψ down to -4.2 MPa (Fig. S7a). While this season was relatively dry with temperature and precipitation in July and August being respectively above- and below-average compared to the decade average (Figs. S7b and S7c), it did not represent an extreme drought year (no branch mortality was observed).

Table 1   Mean values ($\pm$ SE) of water potentials at which 12, 50, and 88% loss of conductivity (microCT and CAVI1000 methods) and loss of embolized pixels (optical technique) occur in stems and leaves of *Laurus nobilis* L. seedlings. S is the slope of the fitted vulnerability curve and corresponds to the speed of embolism spread of a tangent at the inflection point (Ψ_{50}). Letters refer to Bonferroni tests of differences between means

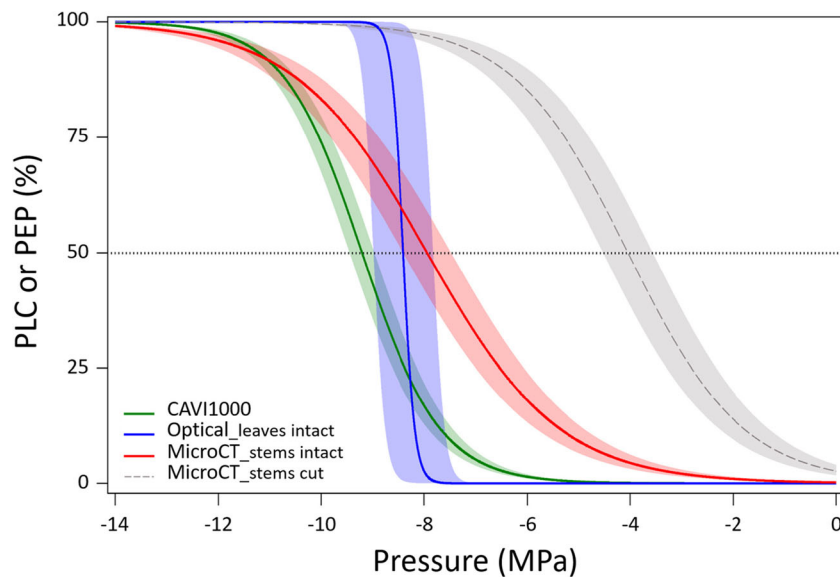| Methods	n	Ψ_{12} (MPa)	Ψ_{50} (MPa)	Ψ_{88} (MPa)	S (% MPa^{-1})
MicroCT					
Intact plants	–	-5.37 ± 0.32ab	-7.94 ± 0.47a	-10.51 ± 0.62ab	19.48 ± 6.13ab
Cut branches	5	-1.60 ± 0.19b	-4.04 ± 0.48b	-6.48 ± 0.77c	22.33 ± 3.14a
CAVI1000	7	-6.94 ± 0.73a	-9.21 ± 0.23a	-11.47 ± 0.35a	32.96 ± 9.00a
Optical					
Midrib	4	-7.45 ± 0.81a	-8.32 ± 0.35a	-9.20 ± 0.52b	273.56 ± 181.44ab
Major veins	4	-8.06 ± 0.19a	-8.49 ± 0.26a	-8.92 ± 0.37b	169.43 ± 55.06a
Minor veins	3	-8.28 ± 0.25a	-8.46 ± 0.34a	-8.64 ± 0.47bc	1230.46 ± 632.26b

Fig. 3 Mean vulnerability curves (VCs) for each of the three independent methods applied on *Laurus nobilis* L. VCs are expressed either as percentage loss of hydraulic conductivity (PLC; microCT and CAVI1000) or percentage of embolized pixels (PEP; optical technique) as a function of xylem pressure. VCs from microCT observations were obtained on intact seedlings and 80-cm cut branches ($n = 5$). The VC generated from the centrifugation (CAVI1000) technique was obtained using 1-m long branches from adult laurels growing on the campus of the University of Bordeaux ($n = 7$). The optical technique was carried out on intact seedlings ($n = 4$). Shaded bands represent standard errors, and 50% loss in conductance is indicated by the horizontal dotted line. Note that the Pammenter model was first fitted per sample before calculating a mean Ψ_{50} and slope per method, with the exception of microCT observations on intact plants for which the model fit was added directly on all the single scans. See Figs. S2, S3, and S4 for corresponding raw data

4 Discussion

Direct visualization of xylem embolism formation in stems and leaves of intact laurels provided strong evidence that this species is much more resistant to embolism than previously reported and illustrates that xylem hydraulic failure in this species only occurs under severe drought (Delzon and Cochard 2014). This finding is consistent with Cochard et al. (2015) whose microCT observations also showed that no drought-induced xylem embolism occurred within the normal operating range of xylem pressures. The seasonal minimum water potential obtained during the summer of 2017 was similar to the water potential causing leaf turgor loss ($\Psi_{tlp} = -3.5$ MPa) observed over the course of a year at two sites in Greece (Rhizopoulou and Mitrakos 1990), which confirms that the drought conditions were moderate that year. It also indicates that even during a moderate dry summer season, laurel reaches water potentials in the field which are much more negative than the Ψ_{50} reported in the previous studies, which would lead to negative hydraulic safety margins. Yet, we found that the seasonal minimum water potential was always higher (less negative) than the Ψ_{50} values obtained in this study on both stems and leaves, suggesting that laurel can potentially sustain significantly drier conditions before hydraulic failure. As a consequence, laurel is expected to display a positive hydraulic safety margin (defined here as the difference between Ψ_{min} and Ψ_{50}) at least under non-extreme drought periods, although such

a margin is known to vary substantially as a function of the variation in soil water potential throughout the species' distribution range (Benito Garzón et al. 2018). Like laurel, other taxa originating from the Tertiary Period tropical and subtropical flora exhibit large positive safety margins with highly embolism-resistant xylem despite seasonal minimum water potentials not approaching Ψ_{50} values. This is for instance the case in the *Callitris* clade where species exhibit extreme Ψ_{50} records (*C. tuberculata*: $\Psi_{50} = -19$ MPa and genus mean $\Psi_{50} = -12$ MPa; Larter et al. 2015; Larter et al. 2017), while midday Ψ values monitored over 2 years at four sites in Australia did not go over -6.2 MPa (Brodribb et al. 2013). These findings are in line with Martin-StPaul et al. (2017) who showed that safety margins increases with increasing embolism resistance.

The high resistance to xylem embolism observed in both seedling and adult laurels is consistent with the fact that this species, like other Mediterranean species, displays thicker intervessel pit membranes compared to species from mesic temperate forests (Jansen et al. 2009). Thick intervessel pit membranes are indeed a critical determinant of embolism resistance in the xylem of angiosperms (Li et al. 2016), probably thanks to their longer pore pathways for air-seeding, while pit membrane thickness will also increase tortuosity (defined as the ratio of the length of a flow path through pit membrane to the width of the pit membrane; Vallabh et al. 2011). Our findings may explain why laurel, contrary to other Tethyan
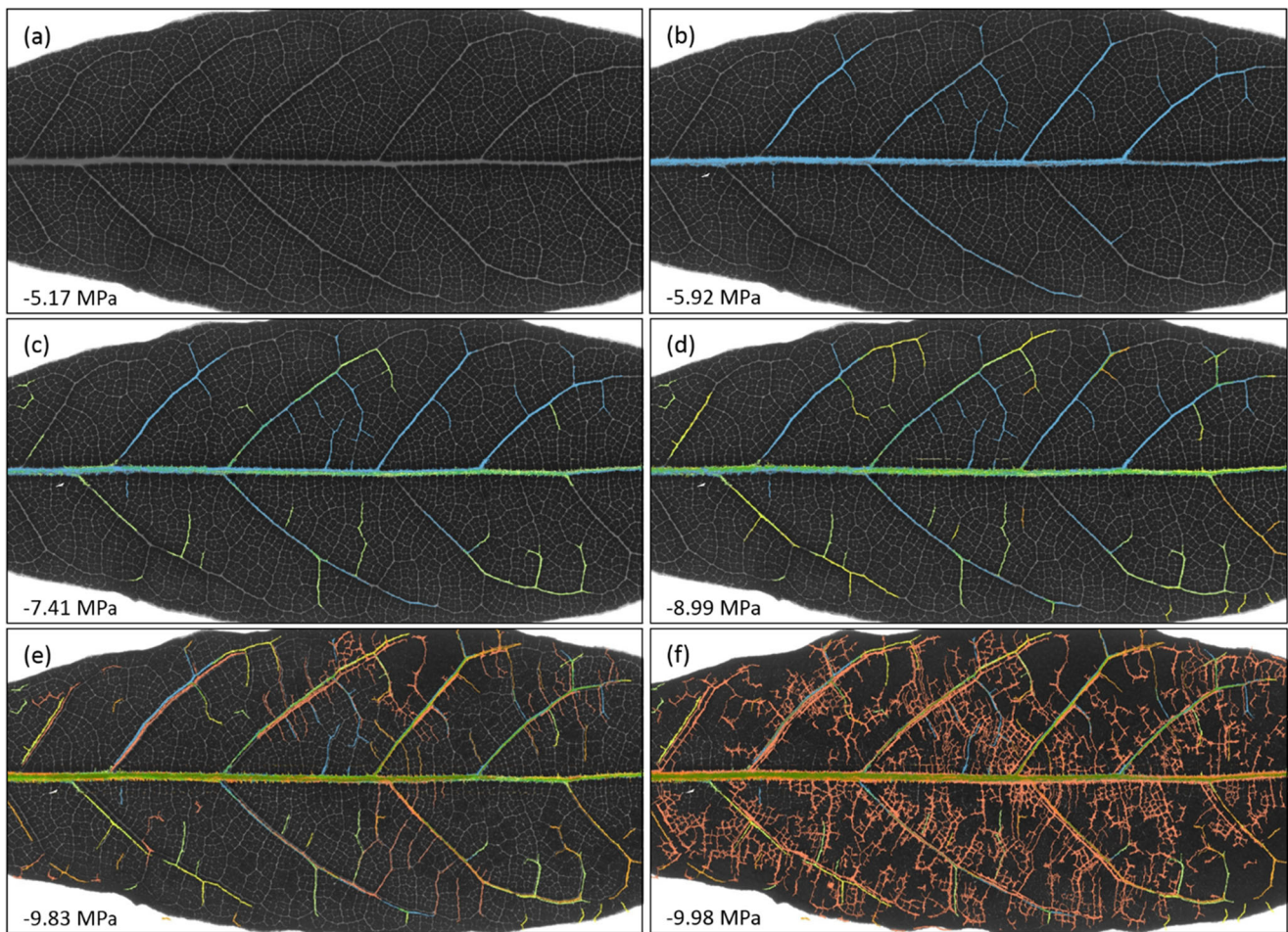
Fig. 4 Digital representation of embolism spread throughout a leaf during the dehydration process of a 3-year-old and 2-m tall intact *Laurus nobilis* seedling. Images **a**–**f** result from the application of the "analyze particles" function on the stack of substracted images (see section 2 for further information on the optical technique image analysis). A color code was applied to represent the whole range of leaf water potential at which embolisms were recorded: blue: −5 to −6 MPa; green: −6 to −7 MPa; green yellow: −7 to −8 MPa; yellow: −8 to −9 MPa; orange: −9 to −9.5 MPa; dark orange: −9.5 to −10 MPa. No embolism was observed until a leaf water potential <−5.17 MPa was reached, which did not occur before 140 h of drying (**a**). The amount of embolism was **b** 6% after 153 h of drying, **c** 11% after 164 h, **d** 16% after 179 h, **e** 61% after 196 h, and **f** 97% after 202 h

Fig. 5 Mean vulnerability curves (VCs) for the different leaf vein orders of *Laurus nobilis* ($n = 4$ for midrib and major (second) veins and $n = 3$ for minor (third and lower order) veins). These VCs were obtained during intact plant dehydration using the optical vulnerability technique (Brodribb et al. 2016). See Fig. S5 for corresponding raw data (i.e., per individual). Shaded bands represent standard errors
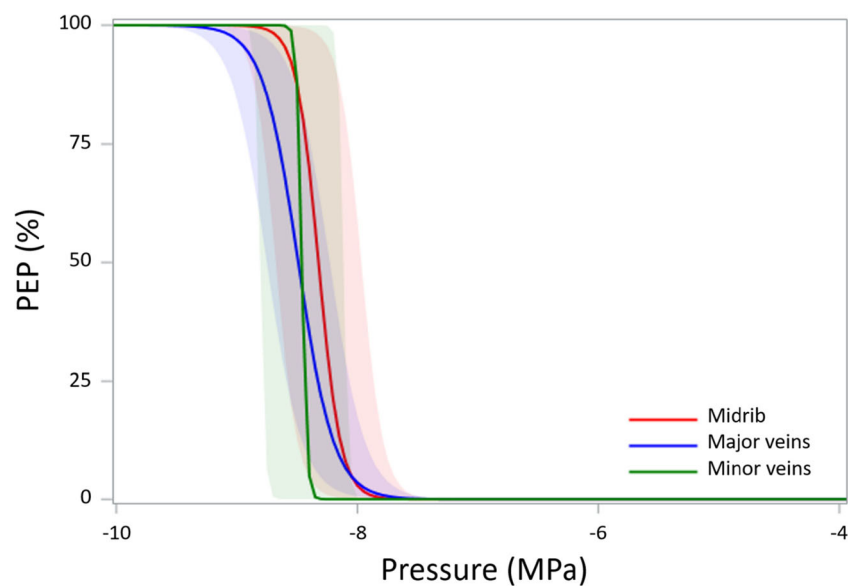
subtropical taxa, succeeded in surviving the climatic fluctuations that occurred since the Pliocene (Svenning 2003), and why it is currently distributed throughout the Mediterranean Basin where drought events are frequent and intense. Finally, our measurements obtained from three independent methods conducted both on stems and leaves converged to the same conclusion that laurel is highly resistant to xylem embolism independently of the development age. The slight difference in Ψ_{50} between laurel seedlings and adults likely results from the use of different plant materials, highlighting a possible ontogenic effect, i.e., increased embolism resistance over the course of plant development, as observed in *Vitis* (Charrier et al. 2018; Choat et al. 2010).

Importantly, our study casts doubts on the reliability of Ψ_{50} values of ca. -2 MPa documented for this species from standard hydraulic methods (Cochard 2002; Hacke and Sperry 2003; Salleo and Lo Gullo 1993; Salleo et al. 1996, 2009). The discrepancy between the Ψ_{50} reported here and these previous studies may be explained by the different artifacts that have been described when determining resistance to embolism of long-vesseled species such as laurel (Choat et al. 2010; Martin-StPaul et al. 2014; Torres-Ruiz et al. 2017; Wheeler et al. 2013; but see Trifilò et al. 2014a, b; Venturas et al. 2015). The use of branches cut shorter than the maximum vessel length for the species can lead to an overestimation of vulnerability to embolism in some species (Torres-Ruiz et al. 2015). Even microCT observations on excised shoots of laurel can result in a less negative Ψ_{50} value of -3.5 (Nardini et al. 2017) and -4.0 MPa (this study), irrespective of the sample length used. In these cases, higher Ψ_{50} values may originate from artifactual increases in the number of embolized vessels caused by the sample preparation, resulting in up to 50% native embolism as observed in Nardini et al. (2017) and for one cut branch in our case. For the four other cut branches in our study, however, the amount of native embolism was low and similar to what was found for intact plants. Higher reported Ψ_{50} values could also be obtained because cut segments may facilitate dehydration of intervessel pit membranes in cut-open vessels, which leads to shrinkage and pit membrane damage and therefore faster spreading of embolism beyond the maximum vessel length (Hillabrand et al. 2016; Li et al. 2016; Zhang et al. 2017). Finally, xylem tension was relaxed in 2-m-long stems prior to sample excision and in situ flow-centrifuge measurements (Torres-Ruiz et al. 2015; Wheeler et al. 2013), leading to a good agreement in the Ψ_{50} value between this hydraulic technique and microCT observations on intact plants. Such proper relaxation cannot be achieved for branches that are desiccated on the bench and regularly scanned on the X-ray stage, adding more uncertainty to the estimation of xylem embolism vulnerability using cut segments.

Another explanation for the difference in Ψ_{50} between this study and previous reports could be intraspecific variability (including genetic differentiation and phenotypic plasticity).

Indeed, phylogeographical reconstructions revealed that refugia within the Mediterranean Basin and Macaronesian Islands helped the species to persist through unsuitable Pleistocene climate, leading to some degree of genetic differentiation between populations (Arroyo-Garcia et al. 2001; Rodríguez-Sánchez et al. 2009). Recent work in this regard has produced mixed results to date, with studies showing little but significant intraspecific variations in *Pinus halepensis* (David-Schwartz et al. 2016) and *Fagus sylvatica* (Schuldt et al. 2016; Stojnic et al. 2018) but not in other species (e.g., in *Pinus pinaster* and four Pinaceae species (Bouche et al. 2016b; Gonzalez-Munoz et al. 2018; Lamy et al. 2011, 2014). However, even when significant intraspecific variability is much lower than the variability between species and is therefore unlikely to explain the more than 6-MPa discrepancy in Ψ_{50} values across studies. Similarly, this large discrepancy is unlikely to originate from the use of different plant materials across experiments. Although previous studies (Cochard 2002; Hacke and Sperry 2003; Salleo et al. 2004; Tyree et al. 1999) were conducted on small and/or young terminal twigs of adult laurels while our data were gathered on plant materials at different development stages (i.e., on both intact seedlings and large branches sampled from adult trees), all our results point toward the same high level of embolism resistance regardless of age.

Our findings bring into question the necessity of a repair mechanism for embolized vessels while xylem is under tension (Nardini et al. 2008; Tyree et al. 1999). Several studies previously suggested that *L. nobilis* can recover from widespread xylem embolism, while water potentials range between -0.5 (Hacke and Sperry 2003) and -1.5 MPa (Salleo et al. 1996; Trifilò et al. 2014b). However, our microCT observations on intact laurels indicate that the level of embolism in stems at such water potentials remains near zero and that no refilling mechanism would be required. In fact, the high level of native xylem embolism (up to 50%) at water potential near 0 MPa reported by Nardini et al. (2017) in branches that were previously rehydrated to favor refilling also suggests an absence of any such refilling. It indicates once again that X-ray observations carried out on short cut segments are not immune to artifactual increases of PLC values during sample preparation. Our results concur with direct microCT observations that xylem refilling is negligible in intact laurel saplings (Knipfer et al. 2017) and does not occur as long as bulk xylem pressure remains negative in *Vitis vinifera* (Charrier et al. 2016). The minimum midday Ψ values down to -4.2 MPa that were recorded over the 2017 summer dry season and the subsequent positive safety margin (i.e., minimum Ψ did not reach Ψ_{50}) displayed by laurel in the field also suggest that embolism formation is unlikely to occur on a daily basis in this species. Overall, real-time, direct X-ray and optical observations in intact plants suggest that previous work that mostly used standard hydraulic techniques (Cochard 2002; Hacke and Sperry 2003; Salleo and Lo Gullo 1993; Salleo et al. 2004; Trifilò et

al. 2014a) or even X-ray microCT (Nardini et al. 2017) on short cut segments likely reported artifactually induced PLCs and refilling. We are consequently not aware of hydraulic studies supporting the existence of refilling in laurel.

Direct visualization of embolized vessels in stems and leaves revealed that xylem vulnerability to embolism (Ψ_{50}) in laurel does not vary among organs. This finding suggests that the difference in embolism resistance between organs within a plant may not be the driving mechanism behind hydraulic segmentation, which posits that the more distal organs, such as leaves and roots, are more vulnerable to embolism than the proximal ones (Zimmermann 1983). A similar xylem embolism resistance across organs has also been reported in the herbaceous *Solanum lycopersicum* (Skelton et al. 2017) and in conifer species (Bouche et al. 2016a, b). However, different results have been found in various conifer species (Sperry and Ikeda 1997) and angiosperm species, such as *Acer grandidentatum* (Alder et al. 1996), *Acer saccharum* (Choat et al. 2005), *Nothofagus* spp. (Bucci et al. 2012), and *V. vinifera* (Charrier et al. 2016; Hochberg et al. 2016). Whether hydraulic segmentation relies on differences in xylem embolism or not remains to be investigated in additional species.

At the leaf level, our results strongly contrast with previous ultrasound acoustic emissions-based measurements of leaf vulnerability to embolism in laurel, which reported a "cavitation threshold" of ca. -0.50 MPa (Salleo et al. 2000, 2001). This discrepancy may be due to the use of cut branches in the aforementioned studies, which led to artifactual increases in the amount of embolism at high water potential. Instead, our results suggest that stomatal closure, which occurs at ca. -2.5 MPa (Salleo et al. 2000), takes place far before embolism initiates, supporting recent findings that plants are generally conservative regarding their water use during drought periods (Hochberg et al. 2017; Martin-StPaul et al. 2017; Skelton et al. 2017). In addition, we found no evidence for differences in vulnerability to embolism among leaf vein orders. This finding is not in line with the first optical vulnerability-based reports, which found that midribs embolize at higher water potentials than lower vein orders in ferns, deciduous species of *Quercus* and herbaceous plants (Brodribb et al. 2016a, b; Scoffoni et al. 2017; Skelton et al. 2017). Differentiation in xylem vulnerability among vein orders in leaves of evergreen angiosperms might differ, and further work should be devoted to this question.

In conclusion, both X-ray microCT and the optical vulnerability technique have recently emerged as prominent techniques to directly evaluate embolism formation in intact plants, thus avoiding artifacts related to embolism determination. While they can be viewed as baseline methods for validating indirect hydraulic measurements and constructing vulnerability curves, they especially offer the possibility to work directly on tall saplings and efficiently assess inter- and intra-organ embolism resistance (i.e., segmentation). Using these techniques on a panel of individuals varying in age, we found

that *L. nobilis* L. is a highly resistant species to drought-induced embolism and that refilling of embolized vessels at relatively high water potentials is unlikely to explain its drought resistance and current geographic distribution. It is also worth noticing that both methods discard non-conductive fluid-filled conduits (i.e., those occluded by gels or tyloses) from analyses. In direct X-ray observations, the percent loss of hydraulic conductivity is calculated from final cuts where only functional vessels are identified, while the optical technique relies on the change in light transmission between water- and gas-filled conduits and thus only highlights water-filled conductive vessels that become embolized through desiccation. The results finally showed that microCT observations are not immune to erroneous PLC determination when short, cut stem samples are used. Caution has to be taken when using short, cut segments, which can be prone to artifacts. We therefore recommend direct quantification of spatial and temporal embolism patterns on intact plants.

Compliance with ethical standards

Conflict of interest The authors declare that they have no competing interests.

References

Alder NN, Sperry JS, Pockman WT (1996) Root and stem xylem embolism, stomatal conductance, and leaf turgor in *Acer grandidentatum* populations along a soil moisture gradient. Oecologia 105:293–301. https://doi.org/10.1007/BF00328731

Allen CD, Macalady AK, Chenchouni H, Bachelet D, McDowell N, Vennetier M, Kitzberger T, Rigling A, Breshears DD, Hogg EH, Gonzalez P, Fensham R, Zhang Z, Castro J, Demidova N, Lim J-H, Allard G, Running SW, Semerci A, Cobb N (2010) A global overview of drought and heat-induced tree mortality reveals

emerging climate change risks for forests. For Ecol Manag 259:660–684. https://doi.org/10.1016/j.foreco.2009.09.001

Allen CD, Breshears DD, McDowell NG (2015) On underestimation of global vulnerability to tree mortality and forest die-off from hotter drought in the Anthropocene. Ecosphere 6:art129. https://doi.org/10.1890/es15-00203.1

Anderegg WRL, Schwalm C, Biondi F, Camarero JJ, Koch G, Litvak M, Ogle K, Shaw JD, Shevliakova E, Williams AP, Wolf A, Ziaco E, Pacala S (2015) Pervasive drought legacies in forest ecosystems and their implications for carbon cycle models. Science 349:528–532. https://doi.org/10.1126/science.aab1833

Anderegg WRL, Martinez-Vilalta J, Cailleret M, Camarero JJ, Ewers BE, Galbraith D, Gessler A, Grote R, C-y H, Levick SR, Powell TL, Rowland L, Sánchez-Salguero R, Trotsiuk V (2016) When a tree dies in the forest: scaling climate-driven tree mortality to ecosystem water and carbon fluxes. Ecosystems 19:1133–1147. https://doi.org/10.1007/s10021-016-9982-1

Arroyo-Garcia R, Martinez-Zapater JM, Fernandez Prieto JA, Alvarez-Arbesu R (2001) AFLP evaluation of genetic similarity among laurel populations (Laurus L.). Euphytica 122:155–164. https://doi.org/10.1023/A:1012654514381

Barigah TS, Charrier O, Douris M, Bonhomme M, Herbette S, Ameglio T, Fichot R, Brignolas F, Cochard H (2013) Water stress-induced xylem hydraulic failure is a causal factor of tree mortality in beech and poplar. Ann Bot 112:1431–1437. https://doi.org/10.1093/aob/mct204

Benito Garzón M, Gonzalez Munoz N, Wigneron J-P, Moisy C, Fernandez-Manjarres J, Delzon S (2018) The legacy of water deficit on populations having experienced negative hydraulic safety margin. Glob Ecol Biogeogr 27:346–356. https://doi.org/10.1111/geb.12701

Bouche PS, Delzon S, Choat B, Badel E, Brodribb TJ, Burlett R, Cochard H, Charra-Vaskou K, Lavigne B, Li S, Mayr S, Morris H, Torres-Ruiz JM, Zufferey V, Jansen S (2016a) Are needles of Pinus pinaster more vulnerable to xylem embolism than branches? New insights from X-ray computed tomography. Plant Cell Environ 39:860–870. https://doi.org/10.1111/pce.12680

Bouche PS, Jansen S, Sabalera JC, Cochard H, Burlett R, Delzon S (2016b) Low intra-tree variability in resistance to embolism in four Pinaceae species. Ann For Sci 73:681–689. https://doi.org/10.1007/s13595-016-0553-6

Brodersen CR, McElrone AJ, Choat B, Matthews MA, Shackel KA (2010) The dynamics of embolism repair in xylem: in vivo visualizations using high-resolution computed tomography. Plant Physiol 154:1088–1095. https://doi.org/10.1104/pp.110.162396

Brodribb TJ, Cochard H (2009) Hydraulic failure defines the recovery and point of death in water-stressed conifers. Plant Physiol 149:575–584. https://doi.org/10.1104/pp.108.129783

Brodribb TJ, Bowman DJ, Nichols S, Delzon S, Burlett R (2010) Xylem function and growth rate interact to determine recovery rates after exposure to extreme water deficit. New Phytol 188:533–542. https://doi.org/10.1111/j.1469-8137.2010.03393.x

Brodribb TJ, Bowman DMJS, Grierson PF, Murphy BP, Nichols S, Prior LD (2013) Conservative water management in the widespread conifer genus Callitris. AoB Plants 5:plt052. https://doi.org/10.1093/aobpla/plt052

Brodribb TJ, Bienaime D, Marmottant P (2016a) Revealing catastrophic failure of leaf networks under stress. Proc Natl Acad Sci U S A 113:4865–4869. https://doi.org/10.1073/pnas.1522569113

Brodribb TJ, Skelton RP, McAdam SA, Bienaime D, Lucani CJ, Marmottant P (2016b) Visual quantification of embolism reveals leaf vulnerability to hydraulic failure. New Phytol 209:1403–1409. https://doi.org/10.1111/nph.13846

Bucci SJ, Scholz FG, Campanello PI, Montti L, Jimenez-Castillo M, Rockwell FA, Manna LL, Guerra P, Bernal PL, Troncoso O, Enricci J, Holbrook MN, Goldstein G (2012) Hydraulic differences along the water transport system of South American Nothofagus species: do leaves protect the stem functionality? Tree Physiol 32:880–893. https://doi.org/10.1093/treephys/tps054

Cailleret M, Jansen S, Robert EM, Desoto L, Aakala T, Antos JA, Beikircher B, Bigler C, Bugmann H, Caccianiga M, Cada V, Camarero JJ, Cherubini P, Cochard H, Coyea MR, Cufar K, Das AJ, Davi H, Delzon S, Dorman M, Gea-Izquierdo G, Gillner S, Haavik LJ, Hartmann H, Heres AM, Hultine KR, Janda P, Kane JM, Kharuk VI, Kitzberger T, Klein T, Kramer K, Lens F, Levanic T, Linares Calderon JC, Lloret F, Lobo-Do-Vale R, Lombardi F, Lopez Rodriguez R, Makinen H, Mayr S, Meszaros I, Metsaranta JM, Minunno F, Oberhuber W, Papadopoulos A, Peltoniemi M, Petritan AM, Rohner B, Sanguesa-Barreda G, Sarris D, Smith JM, Stan AB, Sterck F, Stojanovic DB, Suarez ML, Svoboda M, Tognetti R, Torres-Ruiz JM, Trotsiuk V, Villalba R, Vodde F, Westwood AR, Wyckoff PH, Zafirov N, Martinez-Vilalta J (2017) A synthesis of radial growth patterns preceding tree mortality. Glob Chang Biol 23:1675–1690. https://doi.org/10.1111/gcb.13535

Charrier G, Torres-Ruiz JM, Badel E, Burlett R, Choat B, Cochard H, Delmas CE, Domec JC, Jansen S, King A, Lenoir N, Martin-StPaul N, Gambetta GA, Delzon S (2016) Evidence for hydraulic vulnerability segmentation and lack of xylem refilling under tension. Plant Physiol 172:1657–1668. https://doi.org/10.1104/pp.16.01079

Charrier G, Delzon S, Domec J-C, Zhang L, Delmas CEL, Merlin I, Corso D, King A, Ojeda H, Ollat N, Prieto J, Scholach T, Skinner P, van Leeuwen C, Gambetta GA (2018) Leaf mortality and a dynamic hydraulic safety margin prevent significant stem embolism in the world's top wine regions during drought. Sci. Adv. 4:eaao6969. https://doi.org/10.1126/sciadv.aao6969

Choat B, Lahr EC, Melcher PJ, Zwieniecki MA, Holbrook NM (2005) The spatial pattern of air seeding thresholds in mature sugar maple trees. Plant Cell Environ 28:1082–1089. https://doi.org/10.1111/j.1365-3040.2005.01336.x

Choat B, Drayton WM, Brodersen C, Matthews MA, Shackel KA, Wada H, McElrone AJ (2010) Measurement of vulnerability to water stress-induced cavitation in grapevine: a comparison of four techniques applied to a long-vesseled species. Plant Cell Environ 33:1502–1512. https://doi.org/10.1111/j.1365-3040.2010.02160.x

Choat B, Jansen S, Brodribb TJ, Cochard H, Delzon S, Bhaskar R, Bucci SJ, Feild TS, Gleason SM, Hacke UG, Jacobsen AL, Lens F, Maherali H, Martinez-Vilalta J, Mayr S, Mencuccini M, Mitchell PJ, Nardini A, Pittermann J, Pratt RB, Sperry JS, Westoby M, Wright IJ, Zanne AE (2012) Global convergence in the vulnerability of forests to drought. Nature 491:752–755. https://doi.org/10.1038/nature11688

Choat B, Badel E, Burlett R, Delzon S, Cochard H, Jansen S (2016) Noninvasive measurement of vulnerability to drought-induced embolism by X-ray microtomography. Plant Physiol 170:273–282. https://doi.org/10.1104/pp.15.00732

Clearwater M, Goldstein G (2005) Embolism repair and long distance transport. In: Holbrook NM, Zwieniecki MA (eds) Vascular transport in plants. Elsevier, Amsterdam, pp 201–220

Cochard H (2002) A technique for measuring xylem hydraulic conductance under high negative pressures. Plant Cell Environ 25:815–819. https://doi.org/10.1046/j.1365-3040.2002.00863.x

Cochard H, Delzon S (2013) Hydraulic failure and repair are not routine in trees. Ann For Sci 70:659–661. https://doi.org/10.1007/s13595-013-0317-5

Cochard H, Damour G, Bodet C, Tharwat I, Poirier M, Améglio T (2005) Evaluation of a new centrifuge technique for rapid generation of xylem vulnerability curves. Physiol Plant 124:410–418. https://doi.org/10.1111/j.1399-3054.2005.00526.x

Cochard H, Tete Barigah S, Kleinhentz M, Eshel A (2008) Is xylem cavitation resistance a relevant criterion for screening drought resistance among Prunus species? J Plant Physiol 165:976–982. https://doi.org/10.1016/j.jplph.2007.07.020

Cochard H, Herbette S, Barigah T, Badel E, Ennajeh M, Vilagrosa A (2010) Does sample length influence the shape of xylem embolism vulnerability curves? A test with the Cavitron spinning technique. Plant Cell Environ 33:1543–1552. https://doi.org/10.1111/j.1365-3040.2010.02163.x

Cochard H, Delzon S, Badel E (2015) X-ray microtomography (micro-CT): a reference technology for high-resolution quantification of xylem embolism in trees. Plant Cell Environ 38:201–206. https://doi.org/10.1111/pce.12391

Cohen S, Bennink J, Tyree M (2003) Air method measurements of apple vessel length distributions with improved apparatus and theory. J Exp Bot 54:1889–1897. https://doi.org/10.1093/jxb/erg202

Dai A (2013) Increasing drought under global warming in observations and models. Nat Clim Chang 3:52–58. https://doi.org/10.1038/nclimate1633

David-Schwartz R, Paudel I, Mizrachi M, Delzon S, Cochard H, Lukyanov V, Badel E, Capdeville G, Shklar G, Cohen S (2016) Indirect evidence for genetic differentiation in vulnerability to embolism in *Pinus halepensis*. Front Plant Sci 7:768. https://doi.org/10.3389/fpls.2016.00768

Delzon S, Cochard H (2014) Recent advances in tree hydraulics highlight the ecological significance of the hydraulic safety margin. New Phytol 203:355–358. https://doi.org/10.1111/nph.12798

Dierick M, Masschaele B, Van Hoorebeke L (2004) Octopus, a fast and user-friendly tomographic reconstruction package developed in LabView®. Meas Sci Technol 15:1366–1370. https://doi.org/10.1088/0957-0233/15/7/020

Diffenbaugh NS, Swain DL, Touma D (2015) Anthropogenic warming has increased drought risk in California. Proc Natl Acad Sci U S A 112:3931–3936. https://doi.org/10.1073/pnas.1422385112

Fields CB, Barros V, Stocker TF, Qin D, Dokken DJ, Ebi KL, Mastrandrea MD, Mach KJ, Plattner GK, Allen SK, Tignor M, Midgley PM (2012) Managing the risks of extreme events and disasters to advance climate change adaptation. In: A special report of working groups I and II of the Intergovernmental Panel on Climate Change. Cambridge University Press, Cambridge

Gonzalez-Munoz N, Sterck F, Torres-Ruiz JM, Petit G, Cochard H, von Arx G, Lintunen A, Caldeira MC, Capdeville G, Copini P, Gebauer R, Gronlund L, Holtta T, Lobo-do-Vale R, Peltoniemi M, Stritih A, Urban J, Delzon S (2018) Quantifying in situ phenotypic variability in the hydraulic properties of four tree species across their distribution range in Europe. PLoS One 13:e0196075. https://doi.org/10.1371/journal.pone.0196075

Hacke UG, Sperry JS (2003) Limits to xylem refilling under negative pressure in *Laurus nobilis* and *Acer negundo*. Plant Cell Environ 26:303–311. https://doi.org/10.1046/j.1365-3040.2003.00962.x

Hacke UG, Venturas MD, MacKinnon ED, Jacobsen AL, Sperry JS, Pratt RB (2015) The standard centrifuge method accurately measures vulnerability curves of long-vesselled olive stems. New Phytol 205:116–127. https://doi.org/10.1111/nph.13017

Hillabrand RM, Hacke UG, Lieffers VJ (2016) Drought-induced xylem pit membrane damage in aspen and balsam poplar. Plant Cell Environ 39:2210–2220. https://doi.org/10.1111/pce.12782

Hochberg U, Albuquerque C, Rachmilevitch S, Cochard H, David-Schwartz R, Brodersen CR, McElrone A, Windt CW (2016) Grapevine petioles are more sensitive to drought induced embolism than stems: evidence from in vivo MRI and microcomputed tomography observations of hydraulic vulnerability segmentation. Plant Cell Environ 39:1886–1894. https://doi.org/10.1111/pce.12688

Hochberg U, Windt CW, Ponomarenko A, Zhang YJ, Gersony J, Rockwell FE, Holbrook NM (2017) Stomatal closure, basal leaf embolism, and shedding protect the hydraulic integrity of grape stems. Plant Physiol 174:764–775. https://doi.org/10.1104/pp.16.01816

Hogg E, Brandt J, Michaellian M (2008) Impacts of a regional drought on the productivity, dieback, and biomass of western Canadian aspen forests. Can J For Res 38:1373–1384. https://doi.org/10.1139/X08-001

Jansen S, Choat B, Pletsers A (2009) Morphological variation of intervessel pit membranes and implications to xylem function in angiosperms. Am J Bot 96:409–419. https://doi.org/10.3732/ajb.0800248

Jansen S, Schuldt B, Choat B (2015) Current controversies and challenges in applying plant hydraulic techniques. New Phytol 205:961–964. https://doi.org/10.1111/nph.13229

Jentsch A, Kreyling J, Beierkuhnlein C (2007) A new generation of climate-change experiments: events, not trends. Front Ecol Environ 5:365–374. https://doi.org/10.1890/1540-9295(2007)5[365:ANGOCE]2.0.CO;2

King A, Guignot N, Zerbino P, Boulard E, Desjardins K, Bordessoule M, Leclerq N, Le S, Renaud G, Cerato M, Bornert M, Lenoir N, Delzon S, Perrillat J-P, Legodec Y, Itié J-P (2016) Tomography and imaging at the PSICHE beam line of the SOLEIL synchrotron. Rev Sci Instrum 87:093704. https://doi.org/10.1063/1.4961365

Knipfer T, Cuneo IF, Brodersen CR, McElrone AJ (2016) In situ visualization of the dynamics in xylem embolism formation and removal in the absence of root pressure: a study on excised grapevine stems. Plant Physiol 171:1024–1036. https://doi.org/10.1104/pp.16.00136

Knipfer T, Cuneo IF, Earles JM, Reyes C, Brodersen CR, McElrone AJ (2017) Storage compartments for capillary water rarely refill in an intact woody plant. Plant Physiol 175:1649–1660. https://doi.org/10.1104/pp.17.01133

Lamarque LJ (2018) Data from: an inconvenient truth about xylem resistance to embolism in the model species for refilling *Laurus nobilis* L., Dryad Digital Repository. [Dataset]. https://doi.org/10.5061/dryad.r9q30g0

Lamy JB, Bouffier L, Burlett R, Plomion C, Cochard H, Delzon S (2011) Uniform selection as a primary force reducing population genetic differentiation of cavitation resistance across a species range. PLoS One 6:e23476. https://doi.org/10.1371/journal.pone.0023476

Lamy JB, Delzon S, Bouche PS, Alia R, Vendramin GG, Cochard H, Plomion C (2014) Limited genetic variability and phenotypic plasticity detected for cavitation resistance in a Mediterranean pine. New Phytol 201:874–886. https://doi.org/10.1111/nph.12556

Larter M, Brodribb TJ, Pfautsch S, Burlett R, Cochard H, Delzon S (2015) Extreme aridity pushes trees to their physical limits. Plant Physiol 168:804–807. https://doi.org/10.1104/pp.15.00223

Larter M, Pfautsch S, Domec JC, Trueba S, Nagalingum N, Delzon S (2017) Aridity drove the evolution of extreme embolism resistance and the radiation of conifer genus *Callitris*. New Phytol 215:97–112. https://doi.org/10.1111/nph.14545

Li S, Klepsch M, Jansen S, Schmitt M, Lens F, Karimi Z, Schuldt B, Espino S, Schenk HJ (2016) Intervessel pit membrane thickness as a key determinant of embolism resistance in angiosperm xylem. IAWA J 37:152–171. https://doi.org/10.1163/22941932-20160128

Lindenmayer DB, Laurance WF, Franklin JF (2012) Global decline in large old trees. Science 338:1305–1306. https://doi.org/10.1126/science.1231070

Maherali H, Pockman WT, Jackson RB (2004) Adaptive variation in the vulnerability of woody plants to xylem cavitation. Ecology 85:2184–2199. https://doi.org/10.1890/02-0538

Martin-StPaul N, Longepierre D, Huc R, Delzon S, Burlett R, Joffre R, Rambal S, Cochard H (2014) How reliable are methods to assess xylem vulnerability to cavitation? The issue of 'open vessel' artifact in oaks. Tree Physiol 34:894–905. https://doi.org/10.1093/treephys/tpu059

Martin-StPaul N, Delzon S, Cochard H (2017) Plant resistance to drought depends on timely stomatal closure. Ecol Lett 20:1437–1447. https://doi.org/10.1111/ele.12851

Masschaele B, Dierick M, Van Loo D, Boone MN, Brabant L, Pauwels E, Cnudde V, Van Hoorebeke L (2013) HECTOR: a 240 kV microCT

setup optimized for research. J Phys Conf Ser 463:012012. https://doi.org/10.1088/1742-6596/463/1/012012

McElrone AJ, Choat B, Parkinson D, MacDowell A, Brodersen CR (2013) Utilization of high resolution computed tomography to visualize the three dimensional structure and function of plant vasculature. J Vis Exp 74:50162. https://doi.org/10.3791/50162

Meehl GA, Tebaldi C (2004) More intense, more frequent, and longer lasting heat waves in the 21st century. Science 305:994–997. https://doi.org/10.1126/science.1098704

Michaelian M, Hogg EH, Hall RJ, Arsenault E (2011) Massive mortality of aspen following severe drought along the southern edge of the Canadian boreal forest. Glob Chang Biol 17:2084–2094. https://doi.org/10.1111/j.1365-2486.2010.02357.x

Mirone A, Brun E, Gouillart E, Tafforeau P, Kieffer J (2014) The PyHST2 hybrid distributed code for high speed tomographic reconstruction with interaction reconstruction and a priori knowledge capabilities. Nucl Instrum Methods Phys Res B 324:41–48. https://doi.org/10.1016/j.nimb.2013.09.030

Nardini A, Ramani M, Gortan E, Salleo S (2008) Vein recovery from embolism occurs under negative pressure in leaves of sunflower (*Helianthus annuus*). Physiol Plant 133:755–764. https://doi.org/10.1111/j.1399-3054.2008.01087.x

Nardini A, Savi T, Losso A, Petit G, Pacile S, Tromba G, Mayr S, Trifilò P, Lo Gullo MA, Salleo S (2017) X-ray microtomography observations of xylem embolism in stems of *Laurus nobilis* are consistent with hydraulic measurements of percentage loss of conductance. New Phytol 213:1068–1075. https://doi.org/10.1111/nph.14245

Nolf M, Lopez R, Peters JM, Flavel RJ, Koloadin LS, Young IM, Choat B (2017) Visualization of xylem embolism by X-ray microtomography: a direct test against hydraulic measurements. New Phytol 214:890–898. https://doi.org/10.1111/nph.14462

Paganin D, Mayon SC, Gureyev TE, Miller PR, Wilkins SW (2002) Simultaneous phase and amplitude extraction from a single defocused image of a homogeneous object. J Microsc 206:33–40. https://doi.org/10.1046/j.1365-2818.2002.01010.x

Pammenter NW, Van der Willigen C (1998) A mathematical and statistical analysis of the curves illustrating vulnerability of xylem to cavitation. Tree Physiol 18:589–593. https://doi.org/10.1093/treephys/18.8-9.589

Rhizopoulou S, Mitrakos K (1990) Water relations of evergreen sclerophylls. I. Seasonal changes in the water relations of eleven species from the same environment. Ann Bot 65:171–178. https://doi.org/10.1093/oxfordjournals.aob.a087921

Rockwell FE, Wheeler JK, Holbrook NM (2014) Cavitation and its discontents: opportunities for resolving current controversies. Plant Physiol 164:1649–1660. https://doi.org/10.1104/pp.113.233817

Rodríguez-Sánchez F, Guzmán B, Valido A, Vargas P, Arroyo J (2009) Late Neogene history of the laurel tree (*Laurus* L., Lauraceae) based on phylogeographical analyses of Mediterranean and Macaronesian populations. J Biogeogr 36:1270–1281. https://doi.org/10.1111/j.1365-2699.2009.02091.x

Salleo S, Lo Gullo MA (1993) Drought resistance strategies and vulnerability to cavitation of some Mediterranean sclerophyllous trees. In: Borghetti M, Grace J, Raschi A (eds) Water transport in plants under climate stress. Cambridge University Press, Cambridge, pp 99–113

Salleo S, Lo Gullo MA, de Paoli D, Zippo M (1996) Xylem recovery from cavitation-induced embolism in young plants of *Laurus nobilis*: a possible mechanism. New Phytol 132:47–56. https://doi.org/10.1111/j.1469-8137.1996.tb04507.x

Salleo S, Nardini A, Pitt F, Lo Gullo MA (2000) Xylem cavitation and hydraulic control of stomatal conductance in Laurel (*Laurus nobilis* L.). Plant Cell Environ 23:71–79. https://doi.org/10.1046/j.1365-3040.2000.00516.x

Salleo S, Lo Gullo MA, Raimondo F, Nardini A (2001) Vulnerability to cavitation of leaf minor veins: any impact on leaf gas exchange? Plant Cell Environ 24:851–859. https://doi.org/10.1046/j.0016-8025.2001.00734.x

Salleo S, Lo Gullo MA, Trifilò P, Nardini A (2004) New evidence for a role of vessel-associated cells and phloem in the rapid xylem refilling of cavitated stems of *Laurus nobilis* L. Plant Cell Environ 27:1065–1076. https://doi.org/10.1111/j.1365-3040.2004.01211.x

Salleo S, Trifilò P, Esposito S, Nardini A, Lo Gullo MA (2009) Starch-to-sugar conversion in wood parenchyma of field-growing *Laurus nobilis* plants: a component of the signal pathway for embolism repair? Funct Plant Biol 36:815–825. https://doi.org/10.1071/FP09103

Sanchez-Salguero R, Navarro-Cerrillo RM, Camarero JJ, Fernández-Cancio Á (2012) Selective drought-induced decline of pine species in southeastern Spain. Clim Chang 113:767–785. https://doi.org/10.1007/s10584-011-0372-6

Schuldt B, Knutzen F, Delzon S, Jansen S, Muller-Haubold H, Burlett R, Clough Y, Leuschner C (2016) How adaptable is the hydraulic system of European beech in the face of climate change-related precipitation reduction? New Phytol 210:443–458. https://doi.org/10.1111/nph.13798

Scoffoni C, Albuquerque C, Brodersen CR, Townes SV, John GP, Cochard H, Buckley TN, McElrone AJ, Sack L (2017) Leaf vein xylem conduit diameter influences susceptibility to embolism and hydraulic decline. New Phytol 213:1076–1092. https://doi.org/10.1111/nph.14256

Skelton RP, Brodribb TJ, Choat B (2017) Casting light on xylem vulnerability in an herbaceous species reveals a lack of segmentation. New Phytol 214:561–569. https://doi.org/10.1111/nph.14450

Sperry JS, Pockman WP (1993) Limitation of transpiration by hydraulic conductance and xylem cavitation in *Betula occidentalis*. Plant Cell Environ 16:279–288. https://doi.org/10.1111/j.1365-3040.1993.tb00870.x

Sperry JS, Ikeda T (1997) Xylem cavitation in roots and stems of Douglas-fir and white fir. Tree Physiol. 17:275–280. https://doi.org/10.1093/treephys/17.4.275

Sperry JS, Christman MA, Torres-Ruiz JM, Taneda H, Smith DD (2012) Vulnerability curves by centrifugation: is there an open vessel artefact, and are "r" shaped curves necessarily invalid? Plant Cell Environ 35:601–610. https://doi.org/10.1111/j.1365-3040.2011.02439.x

Stojnic S, Suchocka M, Benito-Garzon M, Torres-Ruiz JM, Cochard H, Bolte A, Cocozza C, Cvjetkovic B, de Luis M, Martinez-Vilalta J, Raebild A, Tognetti R, Delzon S (2018) Variation in xylem vulnerability to embolism in European beech from geographically marginal populations. Tree Physiol 38:173–185. https://doi.org/10.1093/treephys/tpx128

Svenning JC (2003) Deterministic Plio-Pleistocene extinctions in the European cool-temperate tree flora. Ecol Lett 6:646–653. https://doi.org/10.1046/j.1461-0248.2003.00477.x

Tobin MF, Pratt RB, Jacobsen AL, De Guzman M (2013) Xylem vulnerability to cavitation can be accurately characterized in species with long vessels using a centrifuge method. Plant Biol 15:496–504. https://doi.org/10.1111/j.1438-8677.2012.00678.x

Torres-Ruiz JM, Cochard H, Mayr S, Beikircher B, Diaz-Espejo A, Rodriguez-Dominguez CM, Badel E, Fernandez JE (2014) Vulnerability to cavitation in *Olea europaea* current-year shoots: further evidence of an open-vessel artifact associated with centrifuge and air-injection techniques. Physiol Plant 152:465–474. https://doi.org/10.1111/ppl.12185

Torres-Ruiz JM, Jansen S, Choat B, McElrone AJ, Cochard H, Brodribb TJ, Badel E, Burlett R, Bouche PS, Brodersen CR, Li S, Morris H, Delzon S (2015) Direct X-ray microtomography observation confirms the induction of embolism upon xylem cutting under tension. Plant Physiol 167:40–43. https://doi.org/10.1104/pp.114.249706

Torres-Ruiz JM, Cochard H, Mencuccini M, Delzon S, Badel E (2016) Direct observation and modelling of embolism spread between

xylem conduits: a case study in Scots pine. Plant Cell Environ 39: 2774–2785. https://doi.org/10.1111/pce.12840

Torres-Ruiz JM, Cochard H, Choat B, Jansen S, Lopez R, Tomaskova I, Padilla-Diaz CM, Badel E, Burlett R, King A, Lenoir N, Martin-StPaul NK, Delzon S (2017) Xylem resistance to embolism: presenting a simple diagnostic test for the open vessel artefact. New Phytol 215:489–499. https://doi.org/10.1111/nph.14589

Trifilò P, Barbera PM, Raimondo F, Nardini A, Lo Gullo MA (2014a) Coping with drought-induced xylem cavitation: coordination of embolism repair and ionic effects in three Mediterranean evergreens. Tree Physiol 34:109–122. https://doi.org/10.1093/treephys/tpt119

Trifilò P, Raimondo F, Lo Gullo MA, Barbera PM, Salleo S, Nardini A (2014b) Relax and refill: xylem rehydration prior to hydraulic measurements favours embolism repair in stems and generates artificially low PLC values. Plant Cell Environ 37:2491–2499. https://doi.org/10.1111/pce.12313

Tyree MT, Salleo S, Nardini A, Lo Gullo MA, Mosca R (1999) Refilling in embolized vessels in young stems of laurel. Do we need a new paradigm? Plant Physiol 120:11–21. https://doi.org/10.1104/pp.120.1.11

Urli M, Porte AJ, Cochard H, Guengant Y, Burlett R, Delzon S (2013) Xylem embolism threshold for catastrophic hydraulic failure in angiosperm trees. Tree Physiol 33:672–683. https://doi.org/10.1093/treephys/tpt030

Urli M, Lamy J-B, Sin F, Burlett R, Delzon S, Porté AJ (2014) The high vulnerability of Quercus robur to drought at its southern margin paves the way for Quercus ilex. Plant Ecol 216:177–187. https://doi.org/10.1007/s11258-014-0426-8

Vallabh R, Ducoste J, Seyam A-F, Banks-Lee P (2011) Modeling tortuosity in thin fibrous porous media using computational fluid dynamics. J Porous Media 14:791–804. https://doi.org/10.1615/JPorMedia.v14.i9.40

Venturas MD, MacKinnon ED, Jacobsen AL, Pratt RB (2015) Excising stem samples underwater at native tension does not induce xylem cavitation. Plant Cell Environ 38:1060–1068. https://doi.org/10.1111/pce.12461

Vlassenbroeck J, Dierick M, Masschaele B, Cnudde V, Van Hoorebeke L, Jacobs P (2007) Software tools for quantification of X-ray microtomography at the UGCT. Nucl Instrum Methods Phys Res A 580:442–445. https://doi.org/10.1016/j.nima.2007.05.073

Wang R, Zhang L, Zhang S, Cai J, Tyree MT (2014) Water relations of Robinia pseudoacacia L.: do vessels cavitate and refill diurnally or are R-shaped curves invalid in Robinia? Plant Cell Environ 37: 2667–2678. https://doi.org/10.1111/pce.12315

Wheeler JK, Huggett BA, Tofte AN, Rockwell FE, Holbrook NM (2013) Cutting xylem under tension or supersaturated with gas can generate PLC and the appearance of rapid recovery from embolism. Plant Cell Environ 36:1938–1949. https://doi.org/10.1111/pce.12139

Zhang Y, Klepsch M, Jansen S (2017) Bordered pits in xylem of vesselless angiosperms and their possible misinterpretation as perforation plates. Plant Cell Environ 40:2133–2146. https://doi.org/10.1111/pce.13014

Zimmermann MH (1983) Xylem structure and the ascent of sap. Springer, Berlin

Affiliations

Laurent J. Lamarque[1,2] · **Déborah Corso**[2] · **José M. Torres-Ruiz**[2] · **Eric Badel**[3] · **Timothy J. Brodribb**[4] · **Régis Burlett**[2] · **Guillaume Charrier**[2,5] · **Brendan Choat**[6] · **Hervé Cochard**[3] · **Gregory A. Gambetta**[5] · **Steven Jansen**[7] · **Andrew King**[8] · **Nicolas Lenoir**[9] · **Nicolas Martin-StPaul**[10] · **Kathy Steppe**[11] · **Jan Van den Bulcke**[12] · **Ya Zhang**[7] · **Sylvain Delzon**[2]

[1] EGFV, INRA, Univ. Bordeaux, 33882 Villenave d'Ornon, France

[2] BIOGECO, INRA, Univ. Bordeaux, 33615 Pessac, France

[3] Université Clermont-Auvergne, INRA, PIAF, F-63000 Clermont-Ferrand, France

[4] School of Biological Sciences, University of Tasmania, Hobart 7001, Australia

[5] EGFV, INRA, BSA, ISVV, 33882 Villenave d'Ornon, France

[6] Hawkesbury Institute for the Environment, Western Sydney University, Richmond, NSW 2753, Australia

[7] Institute of Systematic Botany and Ecology, Ulm University, Albert-Einstein-Allee 11, 89081 Ulm, Germany

[8] Synchrotron SOLEIL, L'Orme de Merisiers, Saint-Aubin-BP48, 91192 Gif-sur-Yvette Cedex, France

[9] CNRS, University of Bordeaux, UMS 3626 Placamat, F-33608 Pessac, France

[10] URFM, INRA, 84000 Avignon, France

[11] Laboratory of Plant Ecology, Faculty of Bioscience Engineering, Ghent University, Coupure links 653, 9000 Ghent, Belgium

[12] Laboratory of Wood Technology, Department of Forest and Water Management, UGCT-Woodlab-UGent, Ghent University, Coupure Links 653, BE-9000 Ghent, Belgium